Cell Reports
Medicine

Report

A prefrontal thalamocortical readout for conflict-related executive dysfunction in schizophrenia

Graphical abstract

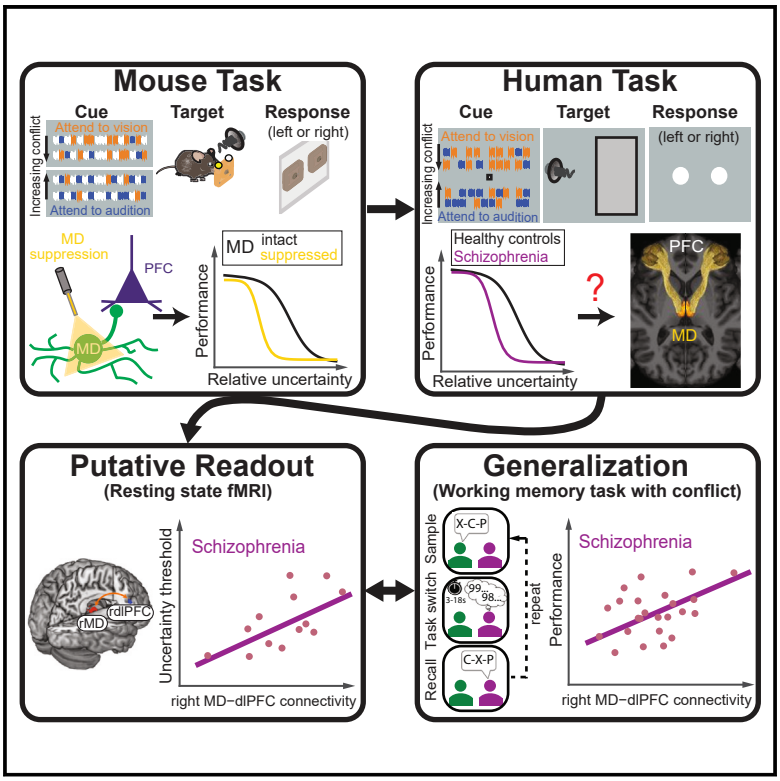

Highlights

- Developed a task to interrogate allocating attention with conflicting inputs
- People with schizophrenia are more susceptible to conflicting inputs
- Right MD-dlPFC functional connectivity as readout for conflict-related executive deficit

Authors

Anna S. Huang, Ralf D. Wimmer, Norman H. Lam, ..., Burkhard Pleger, Michael M. Halassa, Neil D. Woodward

Correspondence

michael.halassa@tufts.edu

In brief

Schizophrenia impairs reasoning and is linked to abnormal interactions between the prefrontal cortex and the mediodorsal thalamus. Huang, Wimmer et al. use behavioral tasks and neuroimaging to uncover this connection, particularly when conflicting information is present. Their findings may lead to biomarkers and future treatments targeting reasoning deficits in schizophrenia.

Huang et al., 2024, Cell Reports Medicine *5*, 101802
November 19, 2024 © 2024 Published by Elsevier Inc.
https://doi.org/10.1016/j.xcrm.2024.101802

CellPress

Cell Reports Medicine

CellPress
OPEN ACCESS

Report

A prefrontal thalamocortical readout for conflict-related executive dysfunction in schizophrenia

Anna S. Huang,[1,6] Ralf D. Wimmer,[2,6] Norman H. Lam,[2] Bin A. Wang,[3,4] Sahil Suresh,[2] Maxwell J. Roeske,[1] Burkhard Pleger,[3,4] Michael M. Halassa,[2,5,7,8,*] and Neil D. Woodward[1,7]

[1]Department of Psychiatry and Behavioral Sciences, Vanderbilt University Medical Center, Nashville, TN, USA
[2]Department of Neuroscience, Tufts University School of Medicine, Boston, MA, USA
[3]Department of Neurology, BG University Hospital Bergmannsheil, Ruhr-University Bochum, Bochum, Germany
[4]Collaborative Research Centre 874 "Integration and Representation of Sensory Processes", Ruhr-University Bochum, Bochum, Germany
[5]Department of Psychiatry, Tufts University School of Medicine, Boston, MA, USA
[6]These authors contributed equally
[7]Senior author
[8]Lead contact
*Correspondence: michael.halassa@tufts.edu
https://doi.org/10.1016/j.xcrm.2024.101802

SUMMARY

Executive dysfunction is a prominent feature of schizophrenia and may drive core symptoms. Dorsolateral prefrontal cortex (dlPFC) deficits have been linked to schizophrenia executive dysfunction, but mechanistic details critical for treatment development remain unclear. Here, capitalizing on recent animal circuit studies, we develop a task predicted to engage human dlPFC and its interactions with the mediodorsal thalamus (MD). We find that individuals with schizophrenia exhibit selective performance deficits when attention is guided by conflicting cues. Task performance correlates with lateralized MD-dlPFC functional connectivity, identifying a neural readout that predicts susceptibility to conflict during working memory in a larger independent schizophrenia cohort. In healthy subjects performing a probabilistic reversal task, this MD-dlPFC network predicts switching behavior. Overall, our three independent experiments introduce putative biomarkers for executive function in schizophrenia and highlight animal circuit studies as inspiration for the development of clinically relevant readouts.

INTRODUCTION

Schizophrenia is a relatively common disorder with worldwide impact.[1] Despite its global impact on affected individuals, their families, and the population at large, its treatment has been relatively stagnant over the last several decades. While the mainstay of treatment is antipsychotic medications, 30% of patients are treatment resistant and almost all exhibit enduring deficits in cognition.[2–5] Collectively, these deficits contribute to poor psychosocial functioning, and their treatment may be central to improving functional outcomes.[6,7]

A vast body of schizophrenia literature connects cognitive impairment to prefrontal cortex (PFC) dysfunction,[8,9] with a specific link between dorsolateral PFC (dlPFC) abnormalities and executive dysfunction.[10] This link is consistent with the basic notion that dlPFC is an area capable of processing complex inputs[11–13] and of projecting the resulting outputs to downstream sensorimotor systems to regulate their ongoing operations.[14–16] This formulation is known as the "top-down" model of dlPFC function.[17,18] While top-down deficits in schizophrenia have been posited,[19] they provide limited insight into a treatment target, in part because of the diversity and breadth of cognitive deficits observed. For example, generalized cognitive impairment characteristic of many patients may not map onto a specific neural system or inform specific treatment targets.[20] This challenge may be addressed by building a mechanistic framework to link specific "latent" cognitive processes with the neural systems most closely responsible for their underlying computations.[21] Therefore, identifying these latent processes, linking them to specific executive functions, and correlating them with computationally inspired brain-based metrics may be a viable first step.

A clue to such computational inspiration is a series of recent basic and clinical discoveries involving the thalamus and its interactions with the PFC.[22–32] Although the thalamus is classically considered to be a sensory relay, recent animal circuit studies have shown that it plays critical non-relay roles in cortical processing.[22,33–38] Specifically, the mediodorsal thalamus (MD), the largest thalamic input to the PFC, is essential for configuring and switching PFC dynamics based on variation in task demands and changes in contingencies within the environment.[34,39–41] Such operations, which rely on MD projections

This is an open access article under the CC BY-NC-ND license (http://creativecommons.org/licenses/by-nc-nd/4.0/).

capable of regulating prefrontal dynamics and effective connectivity,[33,35,42,43] may provide mechanistic inroads for interpreting non-invasive neural measurements in schizophrenia, such as functional magnetic resonance imaging (fMRI). In fact, several groups have already identified changes in temporal correlation in the resting-state blood-oxygenation-level-dependent (BOLD) signal between the thalamus and frontal cortex across multiple schizophrenia cohorts.[24,44] This finding, which is commonly referred to as altered resting-state functional connectivity (dysconnectivity), is of particular importance because it has also been observed in individuals at increased risk for psychosis and may predict conversion to a full-blown psychotic disorder.[25]

Linking these circuit and computational insights to specific executive functions would benefit from task-based fMRI measures, and relatively few studies have examined MD thalamic changes in task contexts. A key challenge to overcome is identifying task conditions that would "drive" MD BOLD responses. Two potential candidates that engage the MD thalamus based on observations in multiple animal studies are changes in stimulus reliability (perceptual uncertainty) on single trials and changes in task rules across multiple trials (contextual uncertainty). For example, rodent studies have shown that the MD thalamus can track uncertainty in perceptual decision-making,[35] and the temporal context in changing environments.[34] Intriguingly, perceptual uncertainty has been shown to drive MD BOLD responses in human subjects performing decision-making tasks,[45] and recent behavioral studies in MD lesion patients have shown a causal relationship between MD function and various components of cognitive flexibility, including task switching.[46,47] Task switching deficits following MD lesions have also been reported in non-human primates.[26,48]

In this study, we started by asking whether uncertainty in deploying executive attention can be used to derive brain-based metrics for executive dysfunction in schizophrenia. To that end, we developed a novel decision-making paradigm in humans based on a previously published rodent task that showed causal requirement but differential contributions of the MD and PFC.[35] Specifically, we asked human subjects to allocate attention to an upcoming auditory or visual target based on single trials, where we parameterized cueing (perceptual) uncertainty and derived behavioral sensitivity measures in a subject-specific manner. We made two critical observations: first, people with schizophrenia demonstrated higher sensitivity to cueing uncertainty than healthy control (HC) participants. Second, this behavioral metric showed a robust and selective correlation with lateralized (right-sided) MD-dlPFC resting-state functional connectivity collected via fMRI in participants performing this task. This right mediodorsal thalamus (rMD)-rdlPFC neural measure predicted executive function in a larger independent sample of participants with schizophrenia, but only when suppressing a conflicting task was required. This commonality with the attentional control task suggests a role for rMD in regulating rdlPFC function when processing conflicting cognitive signals. Indeed, this prediction was further corroborated by a third experiment involving task fMRI. Specifically, in a sample of healthy participants performing a probabilistic rule reversal, we found that the rMD showed robust activation during task switching and that rMD-rdlPFC task-based functional connectivity correlated with switching speed. Our findings therefore suggest that changes in rMD-rdlPFC functional connectivity may represent a readout for executive dysfunction in schizophrenia, particularly in domains requiring prioritization and cognitive resource management.

RESULTS

Participants and clinical characterization of the schizophrenia cohort

We administered a novel decision-making task to a cohort of 24 people with a schizophrenia spectrum disorder diagnosis (i.e., schizophreniform disorder, schizoaffective disorder, and schizophrenia; hereafter referred to as the "schizophrenia group," SZ) and 18 HCs. All participants were administered the Structured Clinical Interview for Diagnostic and Statistical Manual (DSM)-IV/V (SCID) to confirm a schizophrenia spectrum disorder diagnosis in patients and rule out past or current psychiatric illnesses in the HC group. Cognitive ability was measured with the Screen for Cognitive Impairment in Psychiatry (SCIP; Purdon[49]) and the Wechsler Test of Adult Reading (WTAR; 47). In the SZ group, the Positive and Negative Syndrome Scale (PANSS; Kay et al.[50]) was used to characterize and quantify the severity of psychosis symptoms. Demographic characteristics of all participants are presented in Table 1. There was no significant difference between groups in age, sex assigned at birth, race, parental education, or premorbid cognition (as measured with the WTAR). The SZ group had significantly lower education ($T(38) = 2.11$, $p = 0.04$) and current general cognitive abilities (measured with the SCIP composite score) ($T(36) = 3.75$, $p < 0.01$).

Validation of a cross-modal attention task with cueing uncertainty in humans

We developed a novel human decision-making task with cueing uncertainty based on a previously published rodent task, which had revealed the selective causal role for the MD in task performance as a function of cueing uncertainty[35] (Figure S1). In this task, a subject was first instructed that a cue (100 ms bandpass filtered white noise pulse, either high pass [HP] or low pass [LP]) indicated whether an auditory or visual target should be selected (e.g., HP signals "attend to vision"). Subsequently, the cue was turned into a sequence of HP and LP mixtures with varying proportions, where the subject was required to deploy attention based on the predominant pulse type in that sequence (Figure 1A). This design allowed for experimental control over cueing uncertainty on single trials (Figure 1B, example behavioral session). In one-third of the trials, the visual and auditory targets were spatially congruent, while in the other two-thirds they were incongruent. In the HC group ($n = 17$, one was excluded due to poor model fit, see STAR Methods), we found that performance was near flawless and did not vary with cueing uncertainty on congruent trials (Figure 1C, $U = 420$, $p = 0.23$; median ± SD = 0.98 ± 0.01 for low and 0.98 ± 0.02 for high uncertainty; Mann-Whitney U Test, see STAR Methods). Performance was similar regardless of the target modality (Figure 1D, low uncertainty: $U = 331$, $p = 1$; median ± SD = 0.95 ± 0.03 for visual and 0.94 ± 0.04 for auditory trials, high uncertainty: $U = 324$, $p = 0.69$;

CellPress
OPEN ACCESS

Table 1. Demographics for schizophrenia and healthy control groups in experiment 1

	HC (*N* = 18)	SZ (*N* = 24)	T/χ^2	*p* value
Age (years)				
Mean (SD)	29 (±6.4)	27 (±8.0)	0.567	0.574
Sex assigned at birth				
Female	5 (28%)	8 (33%)	0.002	0.962
Male	13 (72%)	16 (67%)	–	–
Race				
Asian	2 (11%)	0 (0%)	5.114	0.276
Black or African American	3 (17%)	2 (8%)	–	–
More than one	2 (11%)	1 (4%)	–	–
Other	1 (6%)	1 (4%)	–	–
White	10 (56%)	20 (83%)	–	–
Education (years)				
Mean (SD)	16 (±2.5)	15 (±2.7)	2.107	0.042
Parental education (years)				
Mean (SD)	15 (±2.2)	16 (±2.3)	−1.208	0.235
Missing	0 (0%)	1 (4.2%)	–	–
SCIP total *Z* score				
Mean (SD)	0.44 (±0.62)	−0.62 (±0.77)	4.755	<0.001
Missing	2 (11.1%)	0 (0%)	–	–
WTAR				
Mean (SD)	110 (±11)	110 (±13)	0.388	0.7
Missing	2 (11.1%)	3 (12.5%)	–	–
PANSS positive				
Mean (SD)	–	14 (±7.3)	–	–
Missing	–	0 (0%)	–	–
PANSS negative				
Mean (SD)	–	13 (±4.8)	–	–
Missing	–	0 (0%)	–	–
PANSS general				
Mean (SD)	–	24 (±6.7)	–	–
Missing	–	0 (0%)	–	–
CPZ equivalents				
Mean (SD)	–	190 (±230)	–	–
Missing	–	1 (4.2%)	–	–

median ± SD = 0.76 ± 0.06 for visual and 0.77 ± 0.06 for auditory trials). In contrast, performance varied with cueing uncertainty in incongruent trials, which was well-fit by a logistic function (Figure 1E).

Reduced tolerance for uncertainty in schizophrenia

Having validated this novel decision-making task, we administered it to the SZ group and found that this group showed performance deficits that scaled with cueing uncertainty (Friedman test: $\chi^2 = 27.22$, $p < 0.01$) (Figures 2A and 2B). This means that SZ subjects had a comparable performance to controls when cues were unambiguous (U = 446, $p = 0.19$; median ± SD = 0.96 ± 0.03 HC; 0.91 ± 0.02 SZ) or of low uncertainty (U = 473, $p = 0.90$; median ± SD = 0.91 ± 0.03 HC; 0.86 ± 0.03 SZ) but showed significantly lower performance with medium- (U = 512, $p = 0.01$; median ± SD = 0.83 ± 0.05 HC; 0.62 ± 0.08 SZ) and high-uncertainty cueing (U = 488.5, $p = 0.01$; median ± SD = 0.65 ± 0.04 HC; 0.54 ± 0.04 SZ). This result was robust to selection for task engagement at either the subject or trial level (Figures S2A and S2B; see STAR Methods). Psychometric functions fit to each subject showed a leftward shift in SZ (Figures 2C and S2C), indicating a lower threshold for (or increased sensitivity to) uncertainty (U = 478, $p < 0.01$; median ± SD = 0.62 ± 0.05 HC; 0.42 ± 0.07 SZ). Importantly, and similar to HC, performance in SZ was comparable between high and low uncertainty on congruent trials (Figure S3A), and SZ subjects performed equivalently for visual and auditory targets (Figure S3B). Increased behavioral sensitivity to cueing uncertainty was unrelated to general cognitive deficits in SZ (Figure S4; WTAR; $F(1,32) = 2.84$, $p = 0.10$).

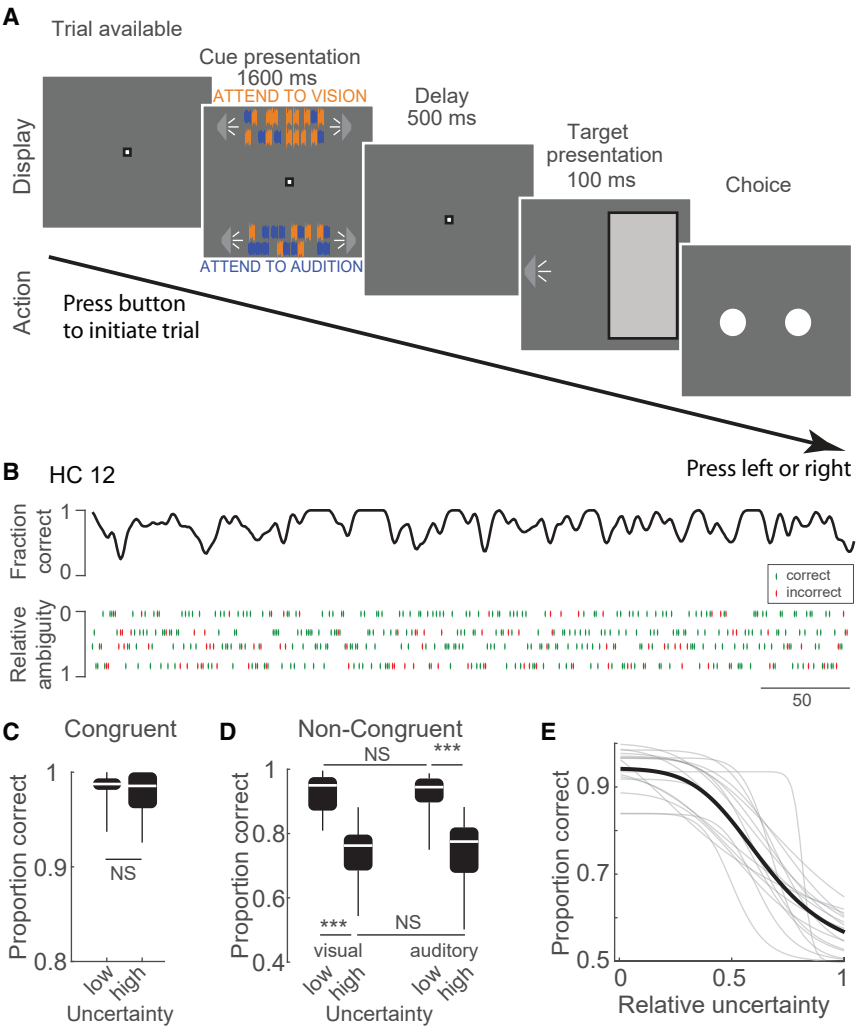

Figure 1. Human subject performance varies with cueing uncertainty in the attentional control task

(A) Task schematic.

(B) Example performance of a healthy control subject showing smoothed performance (top) and correct (green) vs. incorrect (red) behavioral trial raster separated by uncertainty level (bottom).

(C) When visual and auditory targets are presented on the same side (congruent), performance on high and low uncertainty trials is comparable (U = 362, $p = 0.23$, Mann-Whitney U test).

(D) In contrast, when the targets are incongruent, performance varies with cueing uncertainty. Subjects perform equally well on visual and auditory trials (U = 338, $p = 1.00$ and U = 321, $p = 0.69$ for low and high uncertainty, respectively), and performance varies with cueing uncertainty (U = 485, $p < 01$ and U = 476, $p < 0.01$ for vision and audition, respectively) (Mann-Whitney U test).

(E) Psychometric fits for all healthy control subjects (average trace in bold). $N = 17$ subjects for (C–E).

cesses, such as orbitofrontal cortex (Figure S6A, F(1,15) = 0.52, $p = 0.48$). The executive functional specificity was further supported by lack of correlation with the two sensory systems involved in target selection (Figures S6B and S6C). Specifically, no correlation was found between uncertainty threshold with functional connectivity of either primary auditory (F(1,15) = 3.22, $p = 0.09$) or primary visual (F(1,15) = 0.59, $p = 0.46$) thalamocortical loops. Right hemisphere lateralization was also observed in an association of MD volumes with uncertainty thresholds (Figure S7).

Uncertainty thresholds are associated with rMD-rdlPFC functional connectivity

Given that previous rodent studies suggested a role for the MD in tracking uncertainty and regulating executive PFC function accordingly,[42,51,52] we asked if analogous neural mechanisms explained human performance in our decision-making task. As resting-state fMRI was collected in a subgroup of the participants ($n = 20$: HC = 8, SZ = 12), we extracted functional connectivity values between the MD and dlPFC, defined *a priori*. The specific dlPFC region of interest we used in our analysis was based on activation in a task similar to ours in a previous study.[53] We found a significant correlation between uncertainty thresholds and MD and dlPFC functional connectivity that was selective to the right hemisphere (rMD-rdlPFC; Figure 2D, F(1,15) = 6.53, $p = 0.02$, Figure S5). This association significantly differed across hemispheres ($Z = 2.20$, $p = 0.03$, based on Hittner et al.[54]). Brain-behavior correlation was independent of group (SZ vs. HC), and structurally specific to executive PFC, as no correlation was observed with medial PFC structures known to mediate evaluative pro-

rMD-rdlPFC resting-state functional connectivity is predictive of conflict-related executive dysfunction in an independent schizophrenia dataset

The brain-behavior correlation observed in our relatively small cohort was intriguing and compelled us to ask whether the rMD-rdlPFC resting-state functional connectivity measure would be predictive of other forms of executive dysfunction and, if so, what they were. Therefore, we examined a previously collected dataset in which resting-state data were collected alongside a number of standardized neuropsychological tests.[55] The demographic characteristics of participants included in the analysis are summarized in Table 2. Although the neuropsychological tests in this dataset had not been designed to isolate particular cognitive components the way our attentional control task does, we reasoned that their diversity may allow us to discover informative patterns and even draw parallels. Indeed, this was the case; rMD-rdlPFC resting-state functional connectivity was positively correlated with the composite score from the SCIP in SZ (Figure 3A; F(1,65) = 5.56, $p = 0.02$). This correlation was not observed in the left hemisphere (F(1,65) = 1.96, $p = 0.17$).

CellPress
OPEN ACCESS

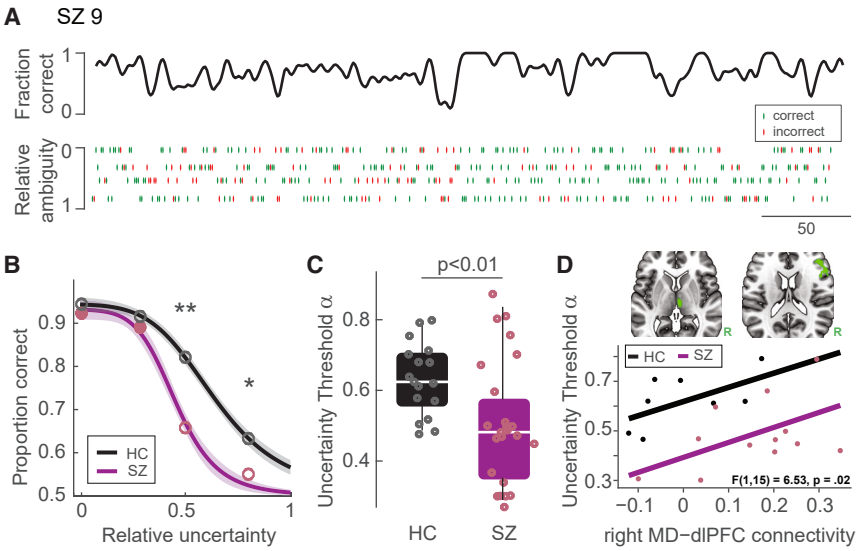

Figure 2. SZ patients show behavioral impairment that scales with cueing uncertainty and correlates with lateralized MD-dlPFC resting-state functional connectivity

(A) Example performance of an SZ subject showing smoothed performance (top) and correct (green) vs. incorrect (red) behavioral trial rasters separated by uncertainty level (bottom).

(B–C) (B) Group comparison of psychometric fits shows lower performance of SZ subjects specifically for trials with higher cueing ambiguity (mean ± SEM, Friedman test: $\chi^2 = 27.22$, $p < 0.01$ followed by pairwise comparison with Mann-Whitney U test, $^{**}p < 0.01$, $^{*}p < 0.05$) resulting in (C) a lower uncertainty threshold for SZ subjects (U = 478, $p < 0.01$, Mann-Whitney U test). $N = 17$ HCs and 24 SZs for (B–C).

(D) There was a positive association between uncertainty thresholds and rMD-rdlPFC across all participants, regardless of group membership ($p = 0.02$). $N = 8$ HCs and 12 SZs.

The SCIP composite score reflects overall performance across a variety of tests assessing multiple different cognitive constructs (e.g., processing speed, working memory, verbal learning), prompting us to examine which component is most responsible for the positive correlation with the rMD-rdlPFC measure. Examining all 5 subdomains (Table S1), the one with the strongest correlation was the SCIP working memory subscale (Figures 3B and 3C). This was a remarkable finding, as the SCIP working memory subscale is a version of the auditory consonant trigrams tests and requires maintaining items in working memory in the face of a conflicting task (digit counting; Figure 3B). Broadly, this offers an intriguing parallel to the conflict observed in the attention task, albeit in the mnemonic instead of perceptual domain. The specificity of the rMD-rdlPFC network isolating conflict-related executive deficits in SZ was further corroborated by the lack of correlation between a separate, conflict-free working memory task (Figure 3D) and rMD-rdlPFC resting-state functional connectivity (Figure 3E).

rMD-rdlPFC network is directly activated in a probabilistic reversal task and predictive of switching speed

Thus far, our work showed that changes in rMD-rdlPFC resting-state functional connectivity correlated with conflict-related executive function. To ask whether this network is directly engaged in resolving conflict, we needed to directly observe it in a task context. Therefore, we turned to the domain of switching between tasks based on reinforcement, a domain that requires active suppression of a task that is no longer rewarding and one in which the MD thalamus has been shown to play a causal role.[28,47] Specifically, we analyzed BOLD signals and brain-behavior correlation in a probabilistic Go/NoGo reversal learning task administered to 32 HCs (Figure 4A). In this task, the association between two tactile cues and two responses (“Go” or “NoGo”) was initially learned over a block of trials.[56] In each block, two new tactile patterns were randomly selected from eight alternative patterns. Because each response yielded a probabilistic reward (0.7 versus 0.3), participants adopted a predominant response pattern within a block. This pattern switched when the association between cues and responses was reversed (Figure 4B). Participants quickly acquired the stimulus-response association and reached maximal performance of around 60% accuracy within 10–15 trials.[56] We focused our analyses on block transitions, which included performance on a well-learned association (steady state) and the learning of a new one (switch).

We applied general linear model analyses to the fMRI data collected in this task, examining activity within the feedback period (trial outcome). Contrasting trials immediately after block transition (switch) with trials immediately before (steady state), we observed significantly enhanced BOLD signals in the right, but not left, MD thalamus (rMD) (Figure 4C, x = 2, y = −14, z = 10, $t^{34} = 6.67$, $p < 0.05$, whole-brain family-wise error [FWE] peak-level correction). In addition to rMD, we also observed switch-related activity in the dorsomedial PFC, caudate, and insular cortex—all located in the right hemisphere ($p < 0.05$, whole-brain FWE peak-level correction).

Next, we performed a psychophysiological interaction (PPI) analysis in HC using the rMD as a seed region (x = 2, y = −14, z = 10, Figure 4D). We found a significant enhancement of rMD-rdlPFC functional connectivity immediately after a switch (rdlPFC, x = 42, y = 20, z = 26, t(31) = 4.37, $p = 0.03$, FWE peak-level corrected using small-volume correction, Figures 4E and 4F). This was not observed on the left hemisphere, consistent with the potential specificity of association between this neural readout and executive function.

To directly test whether this neural readout predicted behavioral performance on this task, we examined the correlation between switch-related rMD-rdlPFC connectivity and the speed to adopt a new strategy. We found this correlation to be significant, with higher network connectivity values reflecting faster

Table 2. Demographics for schizophrenia and healthy control groups in experiment 2

	HC (N = 75)	SZ (N = 70)	T/χ^2	p value
Age				
Mean (SD)	28.3 (8.86)	26.5 (±8.15)	1.28	0.203
Sex assigned at birth				
Female	27 (36.0%)	20 (28.6%)	0.6	0.437
Male	48 (64.0%)	50 (71.4%)	–	–
Race				
Asian	4 (5.3%)	1 (1.4%)	5.75	0.218
Black or African American	16 (21.3%)	18 (25.7%)	–	–
More than one race	1 (1.3%)	0 (0%)	–	–
Other	3 (4.0%)	0 (0%)	–	–
White	51 (68.0%)	51 (72.9%)	–	–
SCIP total score				
Mean (SD)	0.268 (0.605)	−0.850 (0.734)	9.96	<0.001
Missing	–	0 (0%)	–	–
PANSS positive score				
Mean (SD)	–	15.6 (±8.67)	–	–
Missing	–	0 (0%)	–	–
PANSS negative score				
Mean (SD)	–	14.1 (±5.56)	–	–
Missing	–	0 (0%)	–	–
PANSS general score				
Mean (SD)	–	28.4 (±7.54)	–	–
Missing	–	0 (0%)	–	–
CPZ equivalents				
Mean (SD)	–	357 (±196)	–	–
Missing	–	0 (0%)	–	–

switching (Figure 4G, r = −0.36, $p < 0.05$). These findings are consistent with the non-human animal literature showing the causal requirement for the MD in task switching[26,34] but reveals the lateralization of this function in the human brain. Critically, it provides evidence that rMD-rdlPFC functional connectivity is directly deployed in (and may be required for) yet a third conflict-related executive function.

DISCUSSION

Using a novel decision-making task that allowed us to parameterize cueing uncertainty in deploying attention on single trials, we observed that SZ exhibited a specific pattern of behavioral deficit. By deriving psychometric functions from SZ and comparing them to HC, we noted that patients exhibited a higher sensitivity to cueing uncertainty. Individual sensitivity measures correlated with rMD-rdlPFC functional connectivity at rest. This network measure predicted working memory performance in SZ but only when cognitive resources were taxed by a conflicting task. These findings are consistent with predictions from work on animal and human MD, showing its requirement for regulating prefrontal processing when conflict resolution is needed.[34,35,40,45]

Our work extends these findings and adds specificity; the preferential engagement of the right MD-dlPFC network across the three tasks was novel and unexpected. Nonetheless, this finding is consistent with previous literature on preferential rdlPFC engagement in challenging cognitive control tasks.[57–60] Specifically, previous research found that perturbing human right but not left dlPFC function diminished the use of high-level strategies in a reinforcement learning paradigm.[57] While our first two tasks established a link between conflict-related executive control and rdlPFC-rMD resting-state functional connectivity, our third experiment extended that in a task-based paradigm. Specifically, by examining an independent sample of HCs performing a probabilistic reversal learning task, task-based rMD-rdlPFC functional connectivity predicted subject switching speed following reversal.

Our findings are also consistent with previous reports of greater sensitivity to uncertainty when deploying attentional control in schizophrenia[61] and those at clinical high risk for psychosis.[62] Of note, previous literature has also indicated a lateralized dlPFC engagement in this process using continuous performance test.[63,64] Increased sensitivity to uncertainty is broadly supportive of predictive coding models of psychosis, which relate reduced precision of sensory representations (greater uncertainty) and overly precise priors to the severity of hallucinations, and greater volatility with delusions.[65–67] This is also consistent with the "jumping-to-conclusions" phenomenon observed in schizophrenia, whereby SZs "jump" to a decision

CellPress
OPEN ACCESS

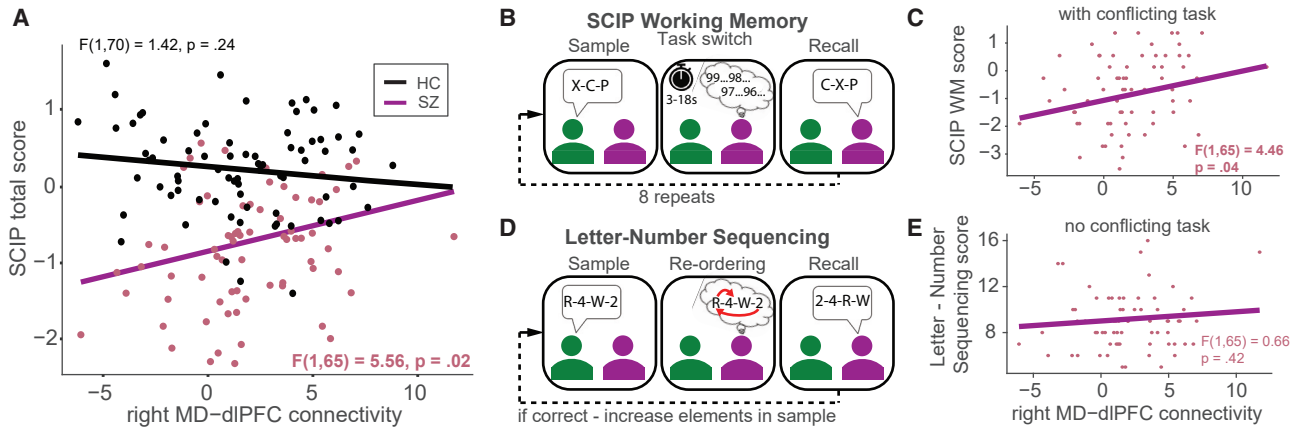

Figure 3. rMD-rdlPFC resting-state functional connectivity is predictive of executive dysfunction in an independent dataset

(A) Association between SCIP scores with rMD-rdlPFC resting-state functional connectivity showed a significant interaction effect ($F(1,138) = 8.00$, $p < 0.01$), showing only a significant positive correlation in the SZ group ($N = 75$ HCs and 70 SZs).

(B) Schematic of the SCIP working memory subscale, illustrating the task conflict component.

(C) rMD-rdlPFC resting-state functional connectivity shows a significant correlation with SCIP working memory subscale performance in SZ ($p = 0.04$).

(D) Schematic of the letter-number sequencing working memory task, where there is no task conflict.

(E) The scores of the letter-number sequencing task do not correlate with rMD-rdlPFC resting-state functional connectivity in SZ ($p = 0.42$).

based on insufficient incoming evidence and are overconfident in their conclusions.[68] Together, our findings add to the evidence that sensitivity to uncertainty is impaired in schizophrenia, with a potential link to cognitive theories of psychosis through impaired allocation of executive (or endogenous) attention.[69]

Most existing paradigms examining uncertainty processing in schizophrenia lack a mechanistic circuit link, making correlational analysis from imaging studies more difficult to interpret. The paradigm we developed here for human subjects was characterized in rodents and shown to rely on mechanisms relevant to MD-dlPFC interactions. Specifically, using causal circuit manipulations and electrophysiological recordings, these studies have identified that MD neurons track perceptual uncertainty and project this cognitive variable onto the prelimbic cortex (rodent analog of primate dlPFC[51,52]). Because the MD contains specialized subcircuits that target inhibitory interneurons (parvalbumin positive), this MD-prelimbic mechanism may afford the ability to slow down decision dynamics in the face of unreliable evidence. Intriguingly, the behavior of SZ (Figure 2C) is qualitatively similar to that observed in mice after MD inactivation (Figures S1B and S1C), and the size of the uncertainty threshold shift in SZ is comparable to the one resulting from MD inactivation in mice. It would be important to ask whether the impairment of such process also generalizes to non-perceptual decisions, potentially explaining phenomena such as bias against disconfirmatory evidence which is also observed in schizophrenia.[70,71]

Our findings indicate that this generality is plausible. Specifically, we found that the rMD-rdlPFC measure positively correlated with working memory processing in the face of a conflicting task, revealed by the SCIP working memory subscale (Figures 3B and 3C). There was no correlation with working memory performance when task conflict was absent (Figures 3D and 3E). Combined, findings across the two datasets indicate that enhanced rMD-rdlPFC functional connectivity may be particularly important for patients with schizophrenia to solve tasks that require managing cognitive resources when there is task conflict/interference (stimulus conflict in the uncertainty task, working memory content in the SCIP subscale). This is consistent with a corpus of neural circuit studies showing a role for the MD in active updating of PFC task representations.[26,34,72] It is also consistent with heightened activation of this network in patients with schizophrenia in a task requiring management of conflicting inputs.[73]

To directly examine rMD-rdlPFC engagement in task BOLD responses, we probed the rMD-rdlPFC network in a probabilistic reversal task (Figure 4). We found that this network showed real-time engagement at rule reversals, another domain that requires conflict resolution. This finding combined with the animal literature spanning related processes supports our circuit/computation → latent cognitive factor → executive function mapping approach. Generally, it provides support for reciprocal interactions between the type of translational research reported in this manuscript and the circuit dissection approach performed in basic neuroscience.[74–82]

While we showed that the rMD-rdlPFC network predicts behavioral performance across three different tasks with a conflict element, there are several limitations that must be considered. First, the imaging data in experiment 1 were small, limiting our ability to correct for multiple comparisons, include additional covariates such as age and sex assigned at birth, and examine the effects of these covariates to increase generalizability of our results. To address this limitation, we sought validation in a larger independent sample of rMD-rdlPFC resting-state connectivity. This (experiment 2) corroborated the notion that conflict-related executive function is associated with rMD-rdlPFC functional connectivity in SZ and allowed us to control for age and sex assigned at birth. However, while the fact that these two experiments use different tasks is a strength on one end, their "offline" nature may be considered a limitation. We did attempt to address this by evaluating the direct engagement of the MD-dlPFC network

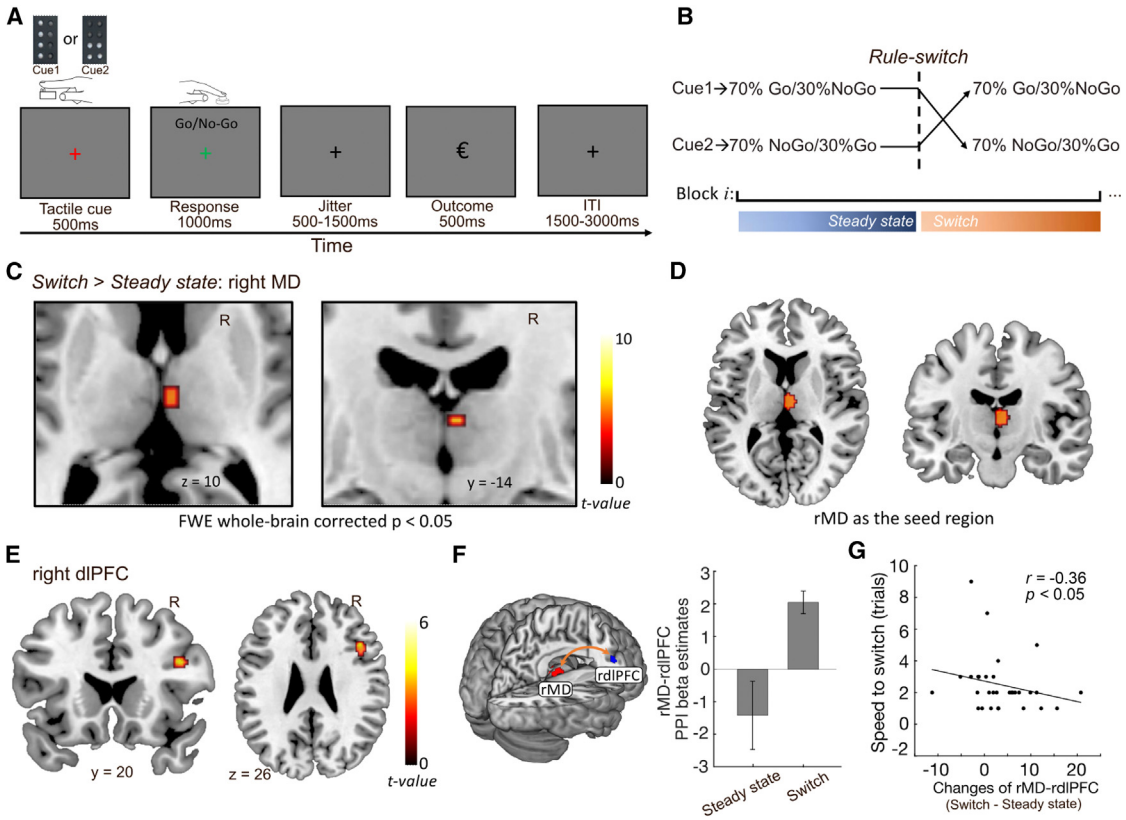

Figure 4. The rMD-rdlPFC network engages in strategy updating

(A) Timeline of the probabilistic Go/NoGo task single trial.

(B) The illustration of a learning block. In each block, 70% of trials in which one of the two tactile patterns was presented were assigned to "Go," whereas 70% of trials in which the alternative tactile pattern was presented were assigned to "NoGo." Within each block, the stimulus-response association was switched at a random trial. The trials immediately before a block transition were categorized as steady state, and the trials immediately after were categorized as switch.

(C) By contrasting switch with steady state, we found significant activity in the right MD (rMD, x = 2, y = −14, z = 10, FWE whole-brain correction, $p < 0.05$).

(D) rMD was used as the seed region for psychophysiological interaction (PPI) analysis.

(E and F) PPI revealed significantly strengthened connectivity between rMD and right dlPFC (x = 24, y = 20, z = 26) immediately after a transition (switch > steady state).

(G) Changes of rMD-rdlPFC PPI estimates (switch – steady state) were negatively correlated with the speed to switch the decision strategy, which suggests that, the more the connectivity between rMD and rdlPFC changed after reversals, the less time (trials) participants required to adapt their behavioral strategy.

in conflict resolution (experiment 3), but that experiment did not include a patient sample which is a limitation. Therefore, it is prudent for future work to examine HC and SZ uncertainty-cued attentional performance in the scanner, where we are able to directly establish online brain-behavior correlations. Lastly, animal circuit work is a strength and motivation—for example, we know that the MD contains circuits that slow down evidence integration as well as those that engage in task switching, linking experiments 1 and 2 with 3[35]; however, we must acknowledge that there are limitations to making inferences to human brain function. Specifically, the lateralization in MD-PFC network function in the human brain likely reflects a unique evolutionary adaptation akin to language, abstract mathematics, and music, all functions that cannot be directly studied in non-human animals, including our closest evolutionary relatives.[83,84]

Despite the aforementioned limitations, our attention task, which incorporated cueing uncertainty, provides a behavioral readout in individuals and connects diminished performance to the integrity of their right MD-dlPFC network. It is therefore possible that this or a similar task may be used as a behavioral screen to identify people with schizophrenia who may benefit from treatments targeting this network. Additional validation might involve strengthening this circuit (e.g., through neuromodulation) and seeing if the ability to resolve uncertainty improves in HC. Together, these directions may inform circuit-based treatments to improve executive function in schizophrenia[85,86] and perhaps ameliorate treatment-resistant psychosis. Consistent with this notion, deep brain stimulation (DBS) of basal ganglia output to the MD has shown promise to reduce hallucinations and unusual thoughts in schizophrenia.[87] DBS use in psychiatric disorders may be difficult; on the other hand, transcarnial magnetic stimulation (TMS) may be a more easily achievable intervention. Irrespective of these trade-offs, our results suggest that the rMD-rdlPFC network may be a viable target for

developing the next-generation neuromodulation targeting endogenous attention and strategy updating in schizophrenia.

Limitations of the study

Experiment 1 included a limited sample size with neuroimaging data, restricting our ability to control for multiple comparisons, include additional demographic variables in our statistical model, and examine the influence of sex assigned at birth on our results leading to limited generalizability of this sample. While the results of experiment 2 corroborated the findings that conflict-related executive functions are associated with rMD-rdlPFC functional connectivity, the tasks used to test conflict-related executive functions were collected outside the scanning session, limiting our ability to examine the direct BOLD responses during conflict processing. Experiment 3 was included to address the direct involvement of rMD-rdlPFC interactions in conflict processing; however, we acknowledge that this experiment did not include a patient sample. Additional experiments directly testing conflict-related executive functions in the MRI comparing HC and schizophrenia groups are needed.

RESOURCE AVAILABILITY

Lead contact

Requests for further information and resources should be directed to and will be fulfilled by the lead contact, Michael Halassa (Michael.Halassa@tufts.edu).

Materials availability

This study did not generate new unique reagents.

Data and code availability

- Animal and limited human data reported in this paper will be shared by the lead contact upon request. As no informed consent for data sharing was obtained for experiment 2, data cannot be shared for that sample.
- This paper does not report original code.
- Any additional information required to reanalyze the data reported in this paper is available from the lead contact upon request.

ACKNOWLEDGMENTS

This work was supported by NIMH grant K24MH126280 and R01 MH102266 (awarded to N.D.W.), 1 P50MH132642 sub-projects 5980 (N.D.W.) and 5978 (M.M.H.), the Charlotte and Donald Test Jr. endowment at VUMC, and the Vanderbilt Institute for Clinical and Translational Research (through grant 1-UL-1-TR000445 from the National Center for Research Resources/NIH). This work was conducted in part using the resources of the Advanced Computing Center for Research and Education (ACCRE) at Vanderbilt University, Nashville, TN. This work was further supported by the Deutsche Forschungsgemeinschaft (DFG, German Research Foundation): project number 122679504 - SFB 874 "Integration and Representation of Sensory Processes" (to B.A.W. and B.P.), project number DFG PL602/6-1 "Prefrontal-thalamic control of cognitive flexibility – from mice to humans" (to B.P.), and the FORUM grant F971-2019 and F1081N-2023 (to B.P.).

AUTHOR CONTRIBUTIONS

M.M.H., N.D.W., A.S.H., and R.D.W. conceptualized the study. A.S.H. and M.J.R. collected and analyzed resting-state data and collected all behavioral data from the uncertainty task. N.H.L., S.S., and R.D.W. analyzed the behavioral data from the uncertainty task. B.A.W. collected and analyzed behavioral and fMRI data of the probabilistic reversal learning task with input from B.P. A.S.H., R.D.W., and M.M.H. wrote the manuscript with input from N.D.W., and all authors read the final version of the manuscript.

DECLARATION OF INTERESTS

The authors declare no competing interests.

STAR★METHODS

Detailed methods are provided in the online version of this paper and include the following:

SUPPLEMENTAL INFORMATION

Supplemental information can be found online at https://doi.org/10.1016/j.xcrm.2024.101802.

Received: January 9, 2024
Revised: June 27, 2024
Accepted: October 2, 2024
Published: November 7, 2024

REFERENCES

1. Solmi, M., Seitidis, G., Mavridis, D., Correll, C.U., Dragioti, E., Guimond, S., Tuominen, L., Dargél, A., Carvalho, A.F., Fornaro, M., et al. (2023). Incidence, prevalence, and global burden of schizophrenia - data, with critical appraisal, from the Global Burden of Disease (GBD) 2019. Mol. Psychiatr. *28*, 5319–5327.
2. Siskind, D., Orr, S., Sinha, S., Yu, O., Brijball, B., Warren, N., MacCabe, J.H., Smart, S.E., and Kisely, S. (2022). Rates of treatment-resistant schizophrenia from first-episode cohorts: systematic review and meta-analysis. Br. J. Psychiatry *220*, 115–120.
3. Meltzer, H.Y. (1997). Treatment-Resistant Schizophrenia - The Role of Clozapine. Curr. Med. Res. Opin. *14*, 1–20.
4. van Os, J., and Kapur, S. (2009). Schizophrenia. Lancet *374*, 635–645.
5. Goff, D.C. (2021). The Pharmacologic Treatment of Schizophrenia-2021. JAMA *325*, 175–176.
6. Anticevic, A., and Halassa, M.M. (2023). The thalamus in psychosis spectrum disorder. Front. Neurosci. *17*, 1163600. https://doi.org/10.3389/fnins.2023.1163600.
7. Mukherjee, A., and Halassa, M.M. (2024). The Associative Thalamus: A Switchboard for Cortical Operations and a Promising Target for Schizophrenia. Neuroscientist *30*, 132–147.
8. Smucny, J., Dienel, S.J., Lewis, D.A., and Carter, C.S. (2022). Mechanisms underlying dorsolateral prefrontal cortex contributions to cognitive

dysfunction in schizophrenia [no. 1]. Neuropsychopharmacology *47*, 292–308.

9. Volk, D.W., and Lewis, D.A. (2010). Prefrontal Cortical Circuits in Schizophrenia. In Behavioral Neurobiology of Schizophrenia and Its Treatment, N.R. Swerdlow, ed. (Berlin, Heidelberg: Springer), pp. 485–508.
10. Perlstein, W.M., Carter, C.S., Noll, D.C., and Cohen, J.D. (2001). Relation of Prefrontal Cortex Dysfunction to Working Memory and Symptoms in Schizophrenia. Aust. J. Pharm. *158*, 1105–1113.
11. Rigotti, M., Barak, O., Warden, M.R., Wang, X.-J., Daw, N.D., Miller, E.K., and Fusi, S. (2013). The importance of mixed selectivity in complex cognitive tasks [no. 7451]. Nature *497*, 585–590.
12. Klein-Flügge, M.C., Bongioanni, A., and Rushworth, M.F.S. (2022). Medial and orbital frontal cortex in decision-making and flexible behavior. Neuron *110*, 2743–2770.
13. Bernardi, S., Benna, M.K., Rigotti, M., Munuera, J., Fusi, S., and Salzman, C.D. (2020). The Geometry of Abstraction in the Hippocampus and Prefrontal Cortex. Cell *183*, 954–967.e21.
14. Plakke, B., Hwang, J., and Romanski, L.M. (2015). Inactivation of Primate Prefrontal Cortex Impairs Auditory and Audiovisual Working Memory. J. Neurosci. *35*, 9666–9675.
15. Kar, K., and DiCarlo, J.J. (2021). Fast Recurrent Processing via Ventrolateral Prefrontal Cortex Is Needed by the Primate Ventral Stream for Robust Core Visual Object Recognition. Neuron *109*, 164–176.e5.
16. Halassa, M.M., and Kastner, S. (2017). Thalamic functions in distributed cognitive control. Nat. Neurosci. *20*, 1669–1679.
17. Miller, E.K., and Cohen, J.D. (2001). An Integrative Theory of Prefrontal Cortex Function. Annu. Rev. Neurosci. *24*, 167–202.
18. Nakajima, M., Schmitt, L.I., and Halassa, M.M. (2019). Prefrontal Cortex Regulates Sensory Filtering through a Basal Ganglia-to-Thalamus Pathway. Neuron *103*, 445–458.e10.
19. Lesh, T.A., Niendam, T.A., Minzenberg, M.J., and Carter, C.S. (2011). Cognitive Control Deficits in Schizophrenia: Mechanisms and Meaning [no. 1]. Neuropsychopharmacology *36*, 316–338.
20. Weickert, T.W., Goldberg, T.E., Gold, J.M., Bigelow, L.B., Egan, M.F., and Weinberger, D.R. (2000). Cognitive Impairments in Patients With Schizophrenia Displaying Preserved and Compromised Intellect. Arch. Gen. Psychiatr. *57*, 907–913.
21. Carter, C.S., and Barch, D.M. (2007). Cognitive Neuroscience-Based Approaches to Measuring and Improving Treatment Effects on Cognition in Schizophrenia: The CNTRICS Initiative. Schizophr. Bull. *33*, 1131–1137.
22. Bolkan, S.S., Stujenske, J.M., Parnaudeau, S., Spellman, T.J., Rauffenbart, C., Abbas, A.I., Harris, A.Z., Gordon, J.A., and Kellendonk, C. (2017). Thalamic projections sustain prefrontal activity during working memory maintenance. Nat. Neurosci. *20*, 987–996.
23. Pergola, G., Danet, L., Pitel, A.-L., Carlesimo, G.A., Segobin, S., Pariente, J., Suchan, B., Mitchell, A.S., and Barbeau, E.J. (2018). The Regulatory Role of the Human Mediodorsal Thalamus. Trends Cognit. Sci. *22*, 1011–1025.
24. Woodward, N.D., and Heckers, S. (2016). Mapping Thalamocortical Functional Connectivity in Chronic and Early Stages of Psychotic Disorders. Biol. Psychiatr. *79*, 1016–1025.
25. Anticevic, A., Haut, K., Murray, J.D., Repovs, G., Yang, G.J., Diehl, C., McEwen, S.C., Bearden, C.E., Addington, J., Goodyear, B., et al. (2015). Association of Thalamic Dysconnectivity and Conversion to Psychosis in Youth and Young Adults at Elevated Clinical Risk. JAMA Psychiatr. *72*, 882–891.
26. Chakraborty, S., Kolling, N., Walton, M.E., and Mitchell, A.S. (2016). Critical role for the mediodorsal thalamus in permitting rapid reward-guided updating in stochastic reward environments. J.I. Gold, ed. *5*, e13588.
27. Nakajima, M., and Halassa, M.M. (2017). Thalamic control of functional cortical connectivity. Curr. Opin. Neurobiol. *44*, 127–131.
28. Rikhye, R.V., Wimmer, R.D., and Halassa, M.M. (2018). Toward an Integrative Theory of Thalamic Function. Annu. Rev. Neurosci. *41*, 163–183.
29. Parnaudeau, S., O'Neill, P.-K., Bolkan, S.S., Ward, R.D., Abbas, A.I., Roth, B.L., Balsam, P.D., Gordon, J.A., and Kellendonk, C. (2013). Inhibition of mediodorsal thalamus disrupts thalamofrontal connectivity and cognition. Neuron *77*, 1151–1162.
30. M.M. Halassa, ed. (2022). *The Thalamus* (Cambridge University Press).
31. Halassa, M.M. (2018). Fronto-thalamic Architectures for Cognitive Algorithms. Neuron *98*, 237–239. https://doi.org/10.1016/j.neuron.2018.04.006.
32. Zhang, X., Halassa, M.M., and Chen, Z.S. (2024). Mediodorsal thalamus regulates sensory and mapping uncertainties in flexible decision making. Preprint at bioRxiv. https://www.biorxiv.org/content/10.1101/2022.12.11.519975v2.full.
33. Schmitt, L.I., Wimmer, R.D., Nakajima, M., Happ, M., Mofakham, S., and Halassa, M.M. (2017). Thalamic amplification of cortical connectivity sustains attentional control [no. 7653]. Nature *545*, 219–223.
34. Rikhye, R.V., Gilra, A., and Halassa, M.M. (2018). Thalamic regulation of switching between cortical representations enables cognitive flexibility [no. 12]. Nat. Neurosci. *21*, 1753–1763.
35. Mukherjee, A., Lam, N.H., Wimmer, R.D., and Halassa, M.M. (2021). Thalamic circuits for independent control of prefrontal signal and noise [no. 7887]. Nature *600*, 100–104.
36. Halassa, M.M., and Sherman, S.M. (2019). Thalamocortical Circuit Motifs: A General Framework. Neuron *103*, 762–770.
37. Wang, M.B., and Halassa, M.M. (2022). Thalamocortical contribution to flexible learning in neural systems. Netw. Neurosci. *6*, 980–997.
38. Hummos, A., Wang, B.A., Drammis, S., Halassa, M.M., and Pleger, B. (2022). Thalamic regulation of frontal interactions in human cognitive flexibility. PLoS Comput. Biol. *18*, e1010500.
39. Roy, D.S., Zhang, Y., Halassa, M.M., and Feng, G. (2022). Thalamic subnetworks as units of function. Nat. Neurosci. *25*, 140–153.
40. Wolff, M., and Halassa, M.M. (2024). The mediodorsal thalamus in executive control. Neuron *112*, 893–908.
41. Zheng, W.-L., Wu, Z., Hummos, A., Yang, G.R., and Halassa, M.M. (2024). Rapid Context Inference in a Thalamocortical Model Using Recurrent Neural Network. Nat. Commun. *15*, 8275.
42. Mukherjee, A., Bajwa, N., Lam, N.H., Porrero, C., Clasca, F., and Halassa, M.M. (2020). Variation of connectivity across exemplar sensory and associative thalamocortical loops in the mouse. Elife *9*, e62554.
43. Scott, D.N., Mukherjee, A., Nassar, M.R., and Halassa, M.M. (2024). Thalamocortical architectures for flexible cognition and efficient learning. Trends Cognit. Sci. *28*, 739–756.
44. Ramsay, I.S. (2019). An Activation Likelihood Estimate Meta-analysis of Thalamocortical Dysconnectivity in Psychosis. Biol. Psychiatry. Cogn. Neurosci. Neuroimaging *4*, 859–869.
45. Kosciessa, J.Q., Lindenberger, U., and Garrett, D.D. (2021). Thalamocortical excitability modulation guides human perception under uncertainty [no. 1]. Nat. Commun. *12*, 2430.
46. Edelstyn, N.M.J., Mayes, A.R., and Ellis, S.J. (2014). Damage to the dorsomedial thalamic nucleus, central lateral intralaminar thalamic nucleus, and midline thalamic nuclei on the right-side impair executive function and attention under conditions of high demand but not low demand. Neurocase *20*, 121–132.
47. Hwang, K., Bruss, J., Tranel, D., and Boes, A.D. (2020). Network Localization of Executive Function Deficits in Patients with Focal Thalamic Lesions. J. Cognit. Neurosci. *32*, 2303–2319.
48. Suthaharan, P., Thompson, S., Rossi-Goldthorpe, R., Rudebeck, P.H., Walton, M., Chakraborty, S., Noonan, M.P., Mitchell, A.S., Costa, V.D., Murray, E.A., et al. (2023). Lesions to the mediodorsal thalamus but not orbitofrontal cortex enhance volatility beliefs linked to paranoia. https://doi.org/10.31234/osf.io/vm78j.

49. Purdon, S. (2005). The Screen for Cognitive Impairment in Psychiatry (SCIP): Instructions and Three Alternate Forms (Edmonton, Alberta: PNL Inc).
50. Kay, S.R., Fiszbein, A., and Opler, L.A. (1987). The Positive and Negative Syndrome Scale (PANSS) for Schizophrenia. Schizophr. Bull. *13*, 261–276.
51. Hoover, W.B., and Vertes, R.P. (2007). Anatomical analysis of afferent projections to the medial prefrontal cortex in the rat. Brain Struct. Funct. *212*, 149–179.
52. Vertes, R.P., Palomero-Gallagher, N., and Halassa, M.M. (2024). The Two Prefrontal Streams: Evidence for Homology across Species (Cambridge (MA): MIT Press).
53. Huang, A.S., Rogers, B.P., and Woodward, N.D. (2019). Disrupted modulation of thalamus activation and thalamocortical connectivity during dual task performance in schizophrenia. Schizophr. Res. *210*, 270–277.
54. Hittner, J.B., May, K., and Silver, N.C. (2003). A Monte Carlo evaluation of tests for comparing dependent correlations. J. Gen. Psychol. *130*, 149–168.
55. Huang, A.S., Rogers, B.P., Anticevic, A., Blackford, J.U., Heckers, S., and Woodward, N.D. (2019). Brain function during stages of working memory in schizophrenia and psychotic bipolar disorder [no. 12]. Neuropsychopharmacology *44*, 2136–2142.
56. Wang, B.A., Veismann, M., Banerjee, A., and Pleger, B. (2023). Human orbitofrontal cortex signals decision outcomes to sensory cortex during behavioral adaptations. Nat. Commun. *14*, 3552.
57. Smittenaar, P., FitzGerald, T.H.B., Romei, V., Wright, N.D., and Dolan, R.J. (2013). Disruption of Dorsolateral Prefrontal Cortex Decreases Model-Based in Favor of Model-free Control in Humans. Neuron *80*, 914–919.
58. Chambers, C.D., Bellgrove, M.A., Gould, I.C., English, T., Garavan, H., McNaught, E., Kamke, M., and Mattingley, J.B. (2007). Dissociable Mechanisms of Cognitive Control in Prefrontal and Premotor Cortex. J. Neurophysiol. *98*, 3638–3647.
59. Swainson, R., Cunnington, R., Jackson, G.M., Rorden, C., Peters, A.M., Morris, P.G., and Jackson, S.R. (2003). Cognitive Control Mechanisms Revealed by ERP and fMRI: Evidence from Repeated Task-Switching. J. Cognit. Neurosci. *15*, 785–799.
60. Spagna, A., Kim, T.H., Wu, T., and Fan, J. (2020). Right hemisphere superiority for executive control of attention. Cortex *122*, 263–276.
61. Weilnhammer, V., Röd, L., Eckert, A.-L., Stuke, H., Heinz, A., and Sterzer, P. (2020). Psychotic Experiences in Schizophrenia and Sensitivity to Sensory Evidence. Schizophr. Bull. *46*, 927–936.
62. Cole, D.M., Diaconescu, A.O., Pfeiffer, U.J., Brodersen, K.H., Mathys, C.D., Julkowski, D., Ruhrmann, S., Schilbach, L., Tittgemeyer, M., Vogeley, K., and Stephan, K.E. (2020). Atypical processing of uncertainty in individuals at risk for psychosis. Neuroimage. Clin. *26*, 102239.
63. Siegel, B.V., Nuechterlein, K.H., Abel, L., Wu, J.C., and Buchsbaum, M.S. (1995). Glucose metabolic correlates of continuous performance test performance in adults with a history of infantile autism, schizophrenics, and controls. Schizophr. Res. *17*, 85–94.
64. Volz, H.-P., Gaser, C., Häger, F., Rzanny, R., Pönisch, J., Mentzel, H.-J., Kaiser, W., and Sauer, H. (1999). Decreased frontal activation in schizophrenics during stimulation with the Continuous Performance Test - a functional magnetic resonance imaging study. Eur. Psychiatr. *14*, 17–24.
65. Corlett, P.R., Horga, G., Fletcher, P.C., Alderson-Day, B., Schmack, K., and Powers, A.R. (2019). Hallucinations and Strong Priors. Trends Cognit. Sci. *23*, 114–127.
66. Feeney, E.J., Groman, S.M., Taylor, J.R., and Corlett, P.R. (2017). Explaining Delusions: Reducing Uncertainty Through Basic and Computational Neuroscience. Schizophr. Bull. *43*, 263–272.
67. Sterzer, P., Voss, M., Schlagenhauf, F., and Heinz, A. (2019). Decision-making in schizophrenia: A predictive-coding perspective. Neuroimage *190*, 133–143.
68. Dudley, R., Taylor, P., Wickham, S., and Hutton, P. (2016). Psychosis, Delusions and the "Jumping to Conclusions'' Reasoning Bias: A Systematic Review and Meta-analysis. Schizophr. Bull. *42*, 652–665.
69. Garety, P.A., Kuipers, E., Fowler, D., Freeman, D., and Bebbington, P.E. (2001). A cognitive model of the positive symptoms of psychosis. Psychol. Med. *31*, 189–195.
70. Woodward, T.S., Moritz, S., Cuttler, C., and Whitman, J.C. (2006). The Contribution of a Cognitive Bias Against Disconfirmatory Evidence (BADE) to Delusions in Schizophrenia. J. Clin. Exp. Neuropsychol. *28*, 605–617.
71. Sanford, N., Veckenstedt, R., Moritz, S., Balzan, R.P., and Woodward, T.S. (2014). Impaired integration of disambiguating evidence in delusional schizophrenia patients. Psychol. Med. *44*, 2729–2738.
72. Phillips, J.M., Afrasiabi, M., Kambi, N.A., Redinbaugh, M.J., Steely, S., Johnson, E.R., Cheng, X., Fayyad, M., Mohanta, S., Caris, A., et al. (2024). Primate thalamic nuclei select abstract rules and shape prefrontal dynamics. Preprint at bioRxiv. https://doi.org/10.1101/2024.03.13.584871.
73. Anticevic, A., Repovs, G., Krystal, J.H., and Barch, D.M. (2012). A broken filter: Prefrontal functional connectivity abnormalities in schizophrenia during working memory interference. Schizophr. Res. *141*, 8–14.
74. Gordon, J.A. (2016). On being a circuit psychiatrist. Nat. Neurosci. *19*, 1385–1386.
75. Rajasethupathy, P., Ferenczi, E., and Deisseroth, K. (2016). Targeting Neural Circuits. Cell *165*, 524–534.
76. Tandon, R., Nasrallah, H., Akbarian, S., Carpenter, W.T., DeLisi, L.E., Gaebel, W., Green, M.F., Gur, R.E., Heckers, S., Kane, J.M., et al. (2024). The schizophrenia syndrome, circa 2024: What we know and how that informs its nature. Schizophr. Res. *264*, 1–28.
77. Dölen, G., Malenka, R.C., Perlmutter, J.S., Brose, N., Frackowiak, R., Cuthbert, B.N., Diester, I., Mansuy, I., Kroker, K.S., Boeckers, T.M., et al. (2015). Pathophysiological Toolkit: Genes to Circuits. In Translational Neuroscience: Toward New Therapies, K. Nikolich and S.E. Hyman, eds. (Cambridge (MA): MIT Press). Retrieved December 22, 2023, from. http://www.ncbi.nlm.nih.gov/books/NBK569711/.
78. Krol, A., Wimmer, R.D., Halassa, M.M., and Feng, G. (2018). Thalamic Reticular Dysfunction as a Circuit Endophenotype in Neurodevelopmental Disorders. Neuron *98*, 282–295.
79. Wells, M.F., Wimmer, R.D., Schmitt, L.I., Feng, G., and Halassa, M.M. (2016). Thalamic reticular impairment underlies attention deficit in Ptchd1(Y/-) mice. Nature *532*, 58–63.
80. Nakajima, M., Schmitt, L.I., Feng, G., and Halassa, M.M. (2019). Combinatorial Targeting of Distributed Forebrain Networks Reverses Noise Hypersensitivity in a Model of Autism Spectrum Disorder. Neuron *104*, 488–500.e11.
81. Wimmer, R.D., Schmitt, L.I., Davidson, T.J., Nakajima, M., Deisseroth, K., and Halassa, M.M. (2015). Thalamic control of sensory selection in divided attention [no. 7575]. Nature *526*, 705–709.
82. Halassa, M.M., Chen, Z., Wimmer, R.D., Brunetti, P.M., Zhao, S., Zikopoulos, B., Wang, F., Brown, E.N., and Wilson, M.A. (2014). State-dependent architecture of thalamic reticular subnetworks. Cell *158*, 808–821. https://doi.org/10.1016/j.cell.2014.06.025.
83. Pittella, J.E.H. (2024). The uniqueness of the human brain: a review. Dement. neuropsychol. *18*, e20230078.
84. Güntürkün, O., Ströckens, F., and Ocklenburg, S. (2020). Brain Lateralization: A Comparative Perspective. Physiol. Rev. *100*, 1019–1063.
85. Geana, A., Barch, D.M., Gold, J.M., Carter, C.S., MacDonald, A.W., Ragland, J.D., Silverstein, S.M., and Frank, M.J. (2022). Using Computational Modeling to Capture Schizophrenia-Specific Reinforcement Learning

Differences and Their Implications on Patient Classification. Biol. Psychiatry. Cogn. Neurosci. Neuroimaging *7*, 1035–1046.

86. Kani, A.S., Shinn, A.K., Lewandowski, K.E., and Öngür, D. (2017). Converging effects of diverse treatment modalities on frontal cortex in schizophrenia: A review of longitudinal functional magnetic resonance imaging studies. J. Psychiatr. Res. *84*, 256–276.
87. Cascella, N., Butala, A.A., Mills, K., Kim, M.J., Salimpour, Y., Wojtasiewicz, T., Hwang, B., Cullen, B., Figee, M., Moran, L., et al. (2021). Deep Brain Stimulation of the Substantia Nigra Pars Reticulata for Treatment-Resistant Schizophrenia: A Case Report. Biol. Psychiatr. *90*, e57–e59.
88. Peirce, J., Gray, J.R., Simpson, S., MacAskill, M., Höchenberger, R., Sogo, H., Kastman, E., and Lindeløv, J.K. (2019). PsychoPy2: Experiments in behavior made easy. Behav Res *51*, 195–203.
89. R Core Team (2023). R: A Language and Environment for Statistical Computing (R Foundation for Statistical Computing).
90. The Mathworks Inc (2023). MATLAB Version: 23.2.0.2391609 (R2023b) Update 2 (The MathWorks Inc.).
91. Gaser, C., Dahnke, R., Thompson, P.M., Kurth, F., and Luders, E.; the Alzheimer's Disease Neuroimaging Initiative (2024). CAT: a computational anatomy toolbox for the analysis of structural MRI data. GigaScience *13*, giae049.
92. Whitfield-Gabrieli, S., and Nieto-Castanon, A. (2012). Conn: A Functional Connectivity Toolbox for Correlated and Anticorrelated Brain Networks. Brain Connect. *2*, 125–141.
93. Su, J.H., Thomas, F.T., Kasoff, W.S., Tourdias, T., Choi, E.Y., Rutt, B.K., and Saranathan, M. (2019). Thalamus Optimized Multi Atlas Segmentation (THOMAS): fast, fully automated segmentation of thalamic nuclei from structural MRI. Neuroimage *194*, 272–282.
94. Vidal, J.P., Danet, L., Péran, P., Pariente, J., Bach Cuadra, M., Zahr, N.M., Barbeau, E.J., and Saranathan, M. (2024). Robust thalamic nuclei segmentation from T1-weighted MRI using polynomial intensity transformation. Brain Struct. Funct. *229*, 1087–1101. https://doi.org/10.1007/s00429-024-02777-5.
95. First, M., Gibbon, M., Spitzer, R., and Williams, J. (1996). User's Guide for the Structured Clinical Interview for DSM-IV axis I Disorders—Research Version (New York: Biometrics Research Department, New York State Psychiatric Institute).
96. First, M.B. (2015). Structured Clinical Interview for the DSM (SCID). The Encyclopedia of Clinical Psychology (John Wiley & Sons, Ltd), pp. 1–6.
97. Wechsler, D. (2001). Wechsler Test of Adult Reading: WTAR (Psychological Corporation).
98. Horton, J.A.M., and Larrabee, G.J. (1999). Wechsler Memory Scale III (Elsevier).
99. Cornblatt, B.A., and Keilp, J.G. (1994). Impaired Attention, Genetics, and the Pathophysiology of Schizophrenia. Schizophr. Bull. *20*, 31–46.
100. Roeske, M.J., McHugo, M., Rogers, B., Armstrong, K., Avery, S., Donahue, M., and Heckers, S. (2024). Modulation of hippocampal activity in schizophrenia with levetiracetam: a randomized, double-blind, crossover, placebo-controlled trial. Neuropsychopharmacology *49*, 681–689.
101. Saranathan, M., Iglehart, C., Monti, M., Tourdias, T., and Rutt, B. (2021). In vivo high-resolution structural MRI-based atlas of human thalamic nuclei. Sci. Data *8*, 275.
102. Maldjian, J.A., Laurienti, P.J., Kraft, R.A., and Burdette, J.H. (2003). An automated method for neuroanatomic and cytoarchitectonic atlas-based interrogation of fMRI data sets. Neuroimage *19*, 1233–1239.
103. Maldjian, J.A., Laurienti, P.J., and Burdette, J.H. (2004). Precentral gyrus discrepancy in electronic versions of the Talairach atlas. Neuroimage *21*, 450–455.

CellPress
OPEN ACCESS

STAR★METHODS

KEY RESOURCES TABLE

REAGENT or RESOURCE	SOURCE	IDENTIFIER
Experimental models: Organisms/strains		
Adult male C57Bl/6 mice, purchased at 8–12 weeks old	Taconic Biosciences	https://www.taconic.com/products/mouse-rat/standard-strains-and-stocks/black-6-b6ntac
Software and algorithms		
Psychopy version 2020.1.3	Peirce et al.,[88]	https://www.psychopy.org/
R version 4.3.1	R Core Team[89]	https://www.r-project.org/
MATLAB versions 2017, 2022b, 2023b	Mathworks[90]	N/A
Statistical Parametric Mapping 12 (SPM12)	https://www.fil.ion.ucl.ac.uk/spm/software/spm12/	https://www.fil.ion.ucl.ac.uk/spm/software/spm12/
Computational Anatomy Toolbox (CAT12)	Gaser et al.,[91]	https://neuro-jena.github.io/cat/
Custom resting state preprocessing script	github.com/baxpr	https://github.com/baxpr/connprep
Custom seed-based connectivity script	github.com/baxpr	https://github.com/baxpr/conncalc
CONN toolbox	Whitfield-Gabrieli & Nieto-Castanon[92]	https://web.conn-toolbox.org/home
Thalamus Optimized Multi Atlas Segmentation (THOMAS)	Saranathan et al.,[93,94]	https://github.com/thalamicseg/hipsthomasdocker
Other		
473-nm and a 556-nm laser to activate iC++ and NpHR3.0, respectively.	Optoengine LLC	https://www.optoengine.com/
200 μm core optic fibers for optical inactivation	Doric Lenses	https://www.doriclenses.com/
3T Philips Intera Achieva MRI scanner	Philips	https://www.usa.philips.com/healthcare/solutions/magnetic-resonance

EXPERIMENTAL MODEL AND STUDY PARTICIPANT DETAILS

Experiment 1

42 participants were recruited; 18 healthy controls (HC) and 24 people with a schizophrenia spectrum disorder diagnosis (i.e., schizophreniform disorder, schizoaffective disorder, schizophrenia; hereafter referred to as the "schizophrenia" (SZ) group). Information about age, sex assigned at birth, racial profile and parental education are available in Table 1. One HC was excluded because the model for behavior failed to converge (performance was too high across all task conditions). Therefore, the final analyzed dataset included 17 HCs and 24 SZ patients. SZ patients were recruited from inpatient and outpatient services at the Vanderbilt Psychiatric Hospital in Nashville, Tennessee. HCs were recruited from Nashville and the surrounding area through advertisement. All participants were administered either the Structured Clinical Interview for Diagnosing (SCID) for DSM-IV[95] or DSM-V[96] Disorders to confirm a schizophrenia spectrum disorder in patients and rule out current or past psychiatric illnesses in healthy individuals. The Positive and Negative Syndrome Scale (PANSS;[50]) was used to further characterize and quantify the severity of psychosis symptoms in patients. Inclusion criteria included: an estimated premorbid IQ > 80, age 18–55 years, not having any medical illnesses that would affect study participation, not being pregnant or lactating, not having a substance use disorder (1-month in patients; lifetime in HCs), not taking any psychotropic drugs (HCs), and not having any MRI contraindications (e.g., metal implants, claustrophobia). Structural MRI scans (n = 37: 16 HC, 21 SZ), resting-state scans (n = 20: 8 HC, 12 SZ) and neurocognitive testing (n = 39: 15 HC, 24 SZ) were also obtained on a subset of participants. This study was approved by the Vanderbilt University Institutional Review Board. All participants provided written informed consent before participating and received financial compensation.

Experiment 2

Data from an independent cohort of 172 individuals (SZ = 96; HC = 76) recruited as part of a previous study [55] was used to investigate the generalization of MD-dlPFC resting-state connectivity associations with cognition. From the independent cohort, 11 were excluded (HC = 1, SZ = 10) for poor scan quality or high motion (FD > 0.5). To reduce heterogeneity in this dataset, an additional 16 SZ were excluded if they were not on antipsychotic medications, or their medication status was uncertain. The final sample

consisted of 75 HC and 70 SZ. Information about age, sex assigned at birth, racial profile and parental education are available in Table 2. Diagnoses of schizophrenia in patients and rule out in healthy individuals was confirmed with the Structured Clinical Interview for Diagnosing DSM-IV Disorders (SCID[96];). Clinical symptoms of psychosis and mania were quantified in patients with the Positive and Negative Syndrome Scale (PANSS;[50]). Exclusion criteria included estimated premorbid IQ of less than 80, age less than 18 or greater than 55, presence of medical illness that would affect study participation (e.g., diabetes, cardiovascular or central nervous system disorder, history of significant head trauma), reported pregnancy or lactation, history of substance abuse/dependence (3-month in patients; lifetime in healthy individuals), psychotropic drug use (healthy individuals), and any MRI contra-indications (e.g., metal implants, claustrophobia). This study was approved by the Vanderbilt University Institutional Review Board and all participants provided written informed consent prior to participating in this study and received financial compensation.

All study participants were administered several neurocognitive tests, including: the Wechsler Test of Adult Reading (WTAR;[97]), a single word-reading test of estimated premorbid intellectual functioning; The Screen for Cognitive Impairment in Psychiatry (SCIP;[49]), a brief test of neuropsychological functioning that assesses verbal learning, WM, processing speed, and verbal fluency; and the Weschler Memory Scale 3rd edition,[98] which consists of the letter number sequencing and spatial span tests.

Experiment 3

Analyses in this study used previously collected data from 32 healthy human participants (16 females, mean age ±SD: 24.5 ± 3.5 years).[56] The study was approved by the local ethics committee of the Ruhr-University Bochum, Germany. All participants gave written informed consent prior to participation. Demographics and the experimental design were described in more detail in [56].

METHOD DETAILS

Experiment 1: Attentional control with cueing uncertainty task

Figure 1A includes a schematic of the attention task with cueing uncertainty. Participants were presented with an auditory cue that consisted of 9 pulses of high- and low-frequency sounds, followed by a brief delay and a stimuli period where both a visual and auditory stimulus were presented simultaneously on the right or left of the screen (visual stimulus) or ear (auditory stimulus). The cue indicated if the participant should respond to the visual or auditory stimulus. Uncertainty was manipulated by varying the ambiguity of the cue, defined as the mixture of high-pass and low-pass cues. Cues were presented with 4 levels of uncertainty: certain, low, medium, and high uncertainty. Participants were instructed to respond to the visual or auditory stimulus depending on which cue (high or low frequency) was most prominent. In one-third of the trials, the visual and auditory stimuli were congruent (appeared on the same side), while in the other two-thirds, the visual and auditory stimuli were incongruent (appeared on opposite sides). We set one-third of the trials as congruent trials to avoid participants adopting a pro-anti strategy, where they only attend to or away from one of the targets. The average task duration was approximately 45 (±5) minutes for HC and 49 (±9) minutes for SZ, including 9 self-paced breaks. The experimental task was coded in Psychopy version 2020.1.3.[88]

Experiment 1: Behavioral model fitting

We analyzed the effect of uncertainty on participants' performance in incongruent trials by fitting a psychometric curve for each individual. This function described the ability of a subject to perform the task across uncertainty levels. It assumes a chance level (50%) performance at the limit of maximum uncertainty (i.e., no sensory evidence), and has three fittable parameters, namely the asymptotic performance in the certain (i.e., infinite sensory evidence) condition (y_{max}), the evidence needed to reach the midpoint of maximum and minimum performance (EC50), and the slope of performance drop with increasing uncertainty (slope):

$$P(c) = 0.5 + (y_{max} - 0.5)\frac{1}{1+10^{-(c-EC50)*slope}}$$

For a first pass analysis, we only included subjects that performed well on the unambiguous trials over the entire session. With a criterion threshold of 65% accuracy, 17 out of 18 HC and 13 out of 24 participants in the SZ group were included in the analysis (Figure S1).

Schizophrenia patients are known for deficits in sustained attention[99] which may have led to general task dis-engagement and contributed to poor overall performance across an entire session. Consistent with this, we observed significant fluctuations in performance of easy trials with consolidated periods of high performance (Figure S1B), suggesting that patients did fully acquire the task rules, but disengaged for some periods during the task. To account for the instability of subjects to engage, we developed an algorithm to identify periods of subject engagement, and only included trials in such periods for further analysis.

Specifically, for each participant we computed a performance score over trials, using the two least ambiguous trial conditions and with a smoothing window of 15 trials. We identified engagement periods iteratively by starting from the trial of the highest performance score and expanding (i.e., including trials before and after) the range until just before the mean performance crosses an accuracy threshold of 80%. Over the remaining trials we repeat the process starting from the trial of the next highest performance score. We continue the process until it cannot define any other periods of a minimum trial length of greater performance. As such this length defines the minimal trial length where an additional error in the next trial will not decrease the performance below the threshold. This allowed us to include 17 HC and 24 SZ subjects for further analysis (see Table S2 for the fraction of trial excluded for each subject).

Mouse data (Figure S1) was collected previously.[35] For optogenetic suppression, animals were injected into PFC and MD with AAV-CamKII-eNPHR3.0-eYFP and AAV-CamKII-IC++-eYFP and light (556nm or 473nm, respectively) was delivered only during the cueing period of the task on a subset of trials and on a trial-by-trial basis. Here, we re-analyzed this data, after bootstrapping for robustness, as described above with single subject psychometric curve fitting for direct comparison with human data.

Experiment 1: Image acquisition and resting-state connectivity processing

Resting-state fMRI scans were acquired from a sub-sample of 20 individuals[100] (HC = 8, SZ = 12) who did the behavioral task. For each individual, a structural T1 and a 5-min resting-state scan were acquired on a Philips 3T scanner. *Structural scan:* High resolution T1-weighted structural scans were acquired with the MPRAGE sequence (voxel size = 1mm^3, TR = 8, FOV = 256 x 156, matrix = 256 x 256; flip angle = 5°). *Resting-state scan:* A 10-min T2*-weighted resting state BOLD scan was acquired for each participant with a single-shot, interleaved, multi-slice, gradient-echo EPI sequence. 300 volumes were acquired with a voxel resolution 3 × 3 × 3.2mm (38 slices, TR/TE = 2000/28ms, FOV = 80 × 80mm, flip angle = 90°).

Resting-state scans were preprocessed in SPM12 (https://www.fil.ion.ucl.ac.uk/spm/). Scans were first slice time corrected, realigned to a mean scan, co-registered with a native space structural scan then normalized to the MNI template using deformation parameters derived from DARTEL normalization in CAT12(91) (https://neuro-jena.github.io/cat/). Denoising and functional connectivity were calculated using the conn toolbox[92] (https://web.conn-toolbox.org/) in MATLAB. Denoising was done with default parameters and included bandpass filtering (0.008–0.9 Hz), regression of CSF and white matter signals, and 12 motion parameters (6 translation and rotation parameters and their first derivative). Framewise displacement (FD) was calculated for all resting-state scans and only scans with a mean FD > 0.5 were included in the analyses. No scans were removed for motion.

After denoising, functional connectivity for each participant was calculated as Pearson's correlations on time-courses extracted from the right MD and dlPFC regions-of-interest (ROIs) described below.

Experiment 1 and 2: Regions-of-interest for functional connectivity analysis

ROIs used in the functional connectivity analysis included separate left and right MD nucleus ROIs derived from the THOMAS atlas in CAT12.[91,101] This atlas is based on manual tracings of multiple thalamic nuclei from white matter nulled structural MRI scans in a 7T scanner.[93] Left and right dlPFC ROIs were derived from a previous study that identified dorsolateral prefrontal cortex clusters that were activated in the comparison of a dual vs. single two alternative forced choice task.[53] These dlPFC ROIs were selected as there were similarities between the task from the previous study and the current task, with both requiring performing choices based on a cue.

Experiment 2: Image acquisition and functional connectivity analysis

Imaging data were collected on a 3T Philips Intera Achieva scanner located at the Vanderbilt University Institute of Imaging Science. High resolution T1 structural scans were collected with a 4.5 min 3D T1 fast field echo sequence with 1 mm^3 isotropic voxels (170 slices, TR/TE = 8.9/4.6, FOV = 256 × 256 × 170 mm, matrix = 256 × 256 × 170, flip angle = 8°). A 10-min T2* weighted resting state echo-planar imaging (EPI) scan was collected with 3 mm^3 isotropic voxels (38 slices, TR/TE = 2000/25 ms, FOV = 240 × 240 mm, matrix = 80 x 80, slice thickness = 3 mm with 0.3 mm gap, flip angle = 90°).

Preprocessing and subject level analyses were carried out using custom code based on SPM12 in MATLAB (https://github.com/baxpr/connprep; https://github.com/baxpr/conncalc). Each study participant's T1 structural scan was segmented into gray matter, white matter, and CSF tissue classes and normalized to Montreal Neurological Institute (MNI) space using CAT12. Functional data underwent motion correction, followed by rigid body registration of the mean functional image to the high resolution T1 image, after non-brain tissue was first removed from the T1. Functional images were then normalized to MNI space using the deformation parameters derived from CAT12 and then smoothed with a 6 mm FWHM Gaussian kernel. Additional denoising of the normalized smoothed images included 0.01–0.10 Hz bandpass filtering and removal of 12 motion parameters (6 motion parameters and their 1st derivatives) as well as 6 principal components of the white matter and CSF.

Functional connectivity for each participant was calculated Pearson's correlations on time-courses extracted from the right MD and dlPFC ROIs used in *Experiment 1*. For statistical analyses, r values were z-transformed.

Experiment 3: Probabilistic reversal learning task

The participants performed a probabilistic reversal learning Go/NoGo task during fMRI scanning (Figure 4A). In each block, two tactile patterns were randomly selected from eight alternative patterns. 70% of trials with one tactile pattern were assigned to 'Go', and 70% of trials with the alternative tactile pattern were assigned to 'NoGo' (Figure 4B). By trial and error, participants had to learn which of the two available responses ('Go' and 'NoGo') had the higher reward probability for each of the two tactile patterns. In each individual block, the association between tactile stimuli and Go/NoGo responses was reversed at a random trial from trial 20 to 25, forcing participants to adjust their behavior to maximize reward (Figure 4B). Participants were informed of the probabilistic nature of the association between tactile stimuli and Go/NoGo responses, as well as the existence of a rule switch in each block, but they were not given information about the levels of probability and the specific timing of the reversal. For each trial, participants first received one out of the two tactile stimulation patterns for 500ms on the index fingertip of the right (dominant) hand. After the tactile cue, the participants had to press the button with the index finger of the left hand ('Go'), or refrain from pressing the button ('NoGo'). After

an interval of 500-1500ms, the outcomes were presented for 500ms to indicate whether the action was correct or wrong. Trials were presented with randomized intertrial interval (ITI) ranging between 1500 and 3000ms in 100ms steps. The task was organized in blocks of 45 trials, and consisted of 3 runs, each included four blocks and lasted about 16min. In total, the fMRI experiment consisted of 540 trials and took about 50mins.

Experiment 3: Image acquisition parameters

The fMRI data for Experiment 3 were obtained using a Philips Achieva 3.0 T X-series scanner equipped with a 32-channel head coil as described in detail in Wang et al., (2023).[56] Functional scans were conducted using a multi-band echo-planar imaging (EPI) sequence with a multi-band acceleration factor of 2. A total of thirty-eight transaxial slices, aligned parallel to the anterior-posterior commissure (AC-PC) and covering the entire brain, were acquired with a voxel size of $2 \times 2 \times 3$ mm^3. The acquisition parameters included a repetition time (TR) of 2,200 ms, an echo time (TE) of 24 ms, a flip angle of 90°, a field of view of 224 mm, and no interslice gap.

Additionally, high-resolution T1-weighted structural images were collected for each participant, comprising 176 transversally oriented slices covering the entire brain. These structural images were used for geometric distortion correction and co-registration with the EPI data. The T1-weighted images were acquired using an isotropic T1 TFE sequence with a voxel size of $1 \times 1 \times 1$ mm^3 and a field of view of 240 x 176 mm^2. Each participant's EPI volumes were preprocessed and analyzed with the Statistical Parametric Mapping software SPM12 (Wellcome Department of Imaging Neuroscience, University College London, UK; http://www.fil.ion.ucl.ac.uk/spm) implemented in MATLAB (R2017b).

Experiment 3: The general linear model (GLM) of fMRI data

The fMRI data preprocessing was described in detail in Wang et al., (2023).[56] In the current study, the preprocessed fMRI data (realigned, normalized, smoothed) was used to conduct a first level general linear model (GLM) time-locked to the onset of the outcome. The GLM included two regressors of interest per block, which accounted for trials in the two key phases of the task (i.e., phase immediately before and phase immediately after the reversals, Steady state and Switch, respectively). The trials in other phases (i.e., phase of initial learning and phase before task completion) and invalid trials (i.e., missing or late responses) were modeled separately. Furthermore, six head motion parameters, as estimated during the realignment procedure, were added as regressors of no interest to minimize false-positive activations due to task-correlated motion. To measure the brain activity related to the effect of the reversal, the fMRI BOLD signal during trials immediately after the reversals (Switch) was contrasted with the fMRI BOLD signal during trials immediately before the reversals (Steady state). The respective t-contrast images for each subject were applied to the group-level one-sample t test ($p < 0.05$, family-wise error (FWE) corrected for the whole brain).

Experiment 3: Psychophysiological interaction (PPI) analysis

To assess context-related differences in functional connectivity of right MD, we performed a PPI analysis using the right MD as the seed region (x = 2, y = −14, z = 10, Figure 4D). First, individual time series of the seed region were extracted from a ROI closest to the nearest local maximum of the group contrast between both contexts (i.e., Switch > Steady state) within a radius of 12 mm. The first Eigenvariate was then calculated across all voxels only located in the right hemisphere and surviving $p = 0.05$ uncorrected within a 6 mm sphere centered on the individual peak voxel. The resulting BOLD time series were adjusted for effects of no interest (e.g., invalid trials and movement parameters) and deconvolved to generate the time series required for constructing first-level GLMs for the PPIs. Then, we examined the effect of the reversals on right MD connectivity. To this end, first-level contrast images were created using the PPI regressor of the interaction between the physiological variable and trials of Steady state, as well as the interaction between the physiological variable and trials of Switch. Next, the contrast images (i.e., Switch > Steady state) were applied to the group-level one-sample t-test. We expected that the immediate effect of reversal was related to interactions between the right MD and right dlPFC. Therefore, we performed a small volume correction (SVC) by restricting the search volume to the right dlPFC mask with a threshold at FWE-corrected peak-level of $p < 0.05$. The right dlPFC mask was defined as Brodmann areas 46 as implemented in the WFU PickAtlas[102,103] based on the results from SZ patients.

QUANTIFICATION AND STATISTICAL ANALYSIS

Experiment 1

We predicted the SZ group ($n = 24$) would have lower uncertainty thresholds than the HC group ($n = 17$). One HC was excluded because the model for behavior failed to converge (performance was too high across all task conditions). To directly compare group performance over different uncertainty levels, we first performed Friedman test with chi-squared (χ^2) test in MATLAB (R2020b), followed by point-to-point comparisons using non-parametric Wilcoxon rank-sum test (Mann Whitney U test) to identify significant differences between the two groups. To account for multiple comparisons, we set the significance threshold of alpha = 0.0125 (Bonferroni correction). Where appropriate, median and standard deviations for each group are reported in the Results.

To examine the association between behavior in the task with cueing uncertainty and MD-dlPFC functional connectivity in R version 4.3.1. We employed a linear regression model, using uncertainty threshold as the dependent variable and MD-dlPFC functional connectivity and group as independent variables, controlling for FD. Initially, we included an interaction term for functional connectivity and group, but after finding it non-significant, we removed it from the model. We used a threshold of $p < 0.05$ for significance

testing. Comparisons of correlation coefficients between functional connectivity and cognition of the left and right hemisphere association was done to test for hemisphere specificity.[54]

Additional exploratory analyses examining the relationship between uncertainty threshold and MD volumes and general cognition are included in the Supplemental Materials.

Experiment 2

Group differences in MD-dlPFC connectivity between the SZ (n = 70) and HC (n = 75) groups were tested with a linear regression model in R version 4.3.1, testing the effect of group on connectivity, controlling for age, sex assigned at birth and FD. From the independent cohort, 11 were excluded (HC = 1, SZ = 10) for poor scan quality or high motion (FD > 0.5). To reduce heterogeneity in this dataset, an additional 16 SZ were excluded if they were not on antipsychotic medications, or their medication status was uncertain.

To measure associations between cognition and functional connectivity in the right MD-dlPFC network in SZ, we ran linear regression models with each cognitive measure (SCIP total score and 5 subscales, and WMI and 2 subscales) as the dependent variable, and functional connectivity as the independent variable, controlling for age, sex assigned at birth and FD in the SZ group. To examine the effect of sex assigned at birth, we ran a separate model with an interaction term for functional connectivity and sex assigned at birth and found that there was no interaction effect for either the SCIP WM task ($F = 0.21$, $p = 0.65$) or the LNS task ($F = 0.56$, $p = 0.46$), so the interaction term was not included in our main analyses. We used a threshold of $p < 0.05$ for significance testing. Comparisons of correlation coefficients between functional connectivity and cognition of the left and right hemisphere association was done to test for hemisphere specificity.[54] Parallel analyses in the healthy group were run as controls and are included in the Supplements.